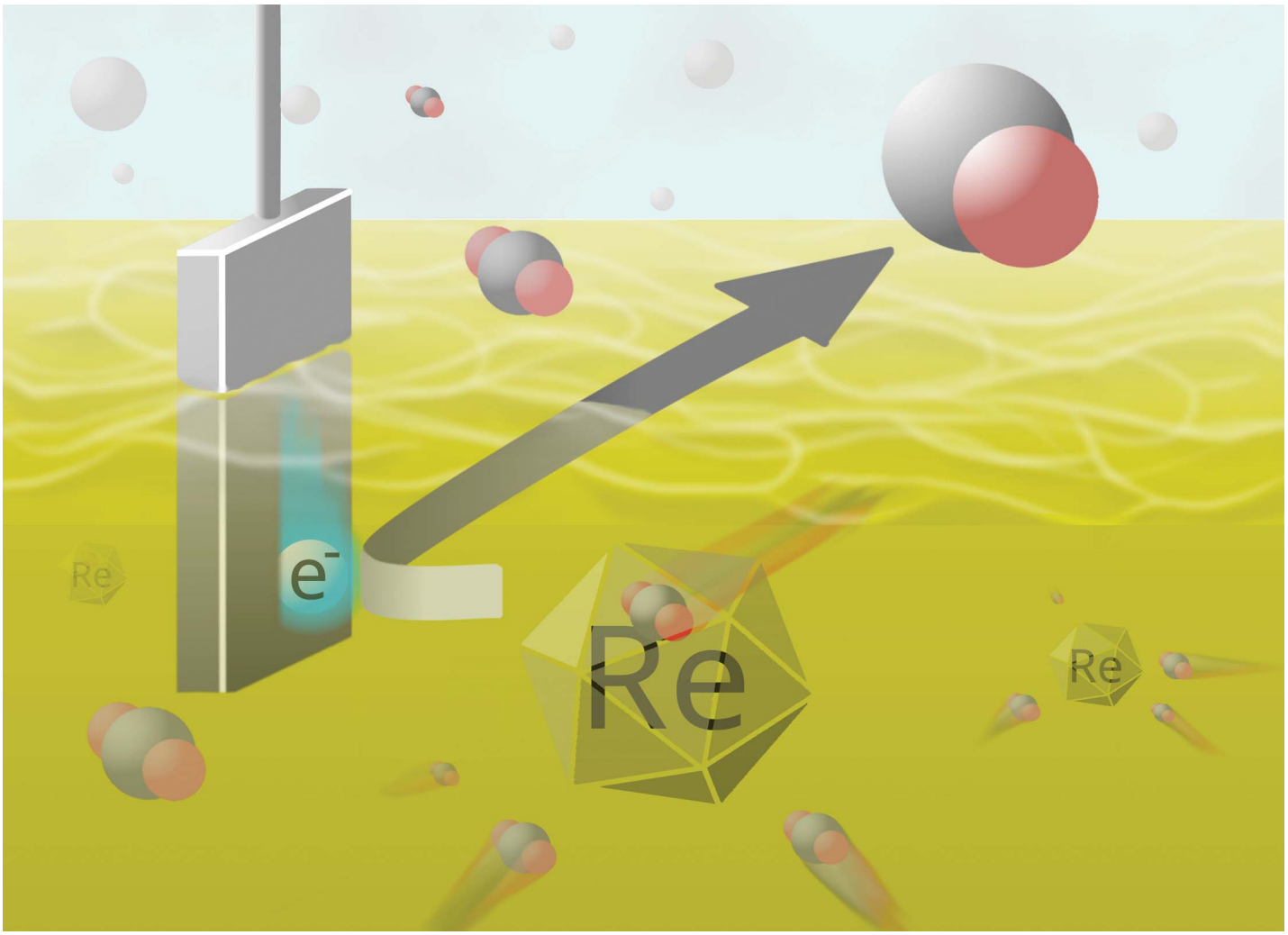

Showcasing research from Professor Ishitani's laboratory, Department of Chemistry, Tokyo Institute of Technology, Tokyo, Japan.

Electrocatalytic reduction of low concentration CO_2

Utilization of low concentration CO_2 contained in the exhaust gases from various industries and thermal power stations without the need for energy-consuming concentration processes should be an important technology for solving global warming and the shortage of fossil resources. Here we report the direct electrocatalytic reduction of low concentration CO_2 by a Re(I)-complex catalyst that possesses CO_2-capturing ability. The reaction rate, the selectivity of CO formation, and Faradaic efficiency were almost the same when using Ar gas containing 10% CO_2 or when using pure CO_2 gas.

As featured in:

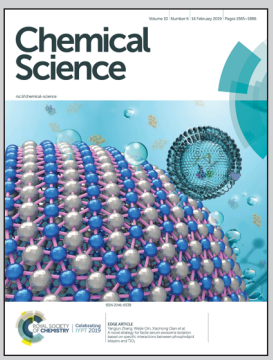

See Osamu Ishitani *et al.*, *Chem. Sci.*, 2019, **10**, 1597.

ROYAL SOCIETY OF CHEMISTRY | Celebrating IYPT 2019

rsc.li/chemical-science

Registered charity number: 207890

Chemical Science

EDGE ARTICLE

View Article Online
View Journal | View Issue

Cite this: *Chem. Sci.*, 2019, **10**, 1597

All publication charges for this article have been paid for by the Royal Society of Chemistry

Received 17th September 2018
Accepted 11th November 2018

DOI: 10.1039/c8sc04124e

rsc.li/chemical-science

Electrocatalytic reduction of low concentration CO_2†

Hiromu Kumagai, ‡ Tetsuya Nishikawa,‡ Hiroki Koizumi, Taiki Yatsu, Go Sahara, Yasuomi Yamazaki, § Yusuke Tamaki and Osamu Ishitani *

Utilization of low concentration CO_2 contained in the exhaust gases from various industries and thermal power stations without the need for energy-consuming concentration processes should be an important technology for solving global warming and the shortage of fossil resources. Here we report the direct electrocatalytic reduction of low concentration CO_2 by a Re(I)-complex catalyst that possesses CO_2-capturing ability in the presence of triethanolamine. The reaction rate and faradaic efficiency of CO_2 reduction were almost the same when using Ar gas containing 10% CO_2 or when using pure CO_2 gas, and the selectivity of CO formation was very high (98% at 10% CO_2). At a concentration of 1% CO_2, the Re(I) complex still behaved as a good electrocatalyst; 94% selectivity of CO formation and 85% faradaic efficiency were achieved, and the rate of CO formation was 67% compared to that when using pure CO_2 gas. The electrocatalysis was due to the efficient insertion of CO_2 into the Re(I)–O bond in *fac*-[Re(dmb)(CO)$_3${$OC_2H_4N(C_2H_4OH)_2$}] (dmb = 4,4′-dimethyl-2,2′-bipyridine).

Introduction

Efforts to solve global warming problems caused by the increasing CO_2 concentration in the atmosphere have focused on carbon capture and storage (CCS). However, the depletion of fossil resources as energy sources and as chemical raw materials is another extended problem. Both of these serious problems have the same origin; there are no practical methods to utilize the large volumes of CO_2 produced in daily life and industrially, as a main carbon source. However, in nature, photosynthesis uses the low concentration of CO_2 in the atmosphere as the carbon source to produce high-energy organic materials using sunlight as an energy source. The electrocatalytic reduction of CO_2 has been widely investigated,[1–5] but most of these reports targeted pure CO_2 despite the fact that exhaust gases from heavy industries only contain low concentrations of CO_2; for example, 3–13% in the case of fire power plants.[6] Although condensation technologies of low concentration CO_2 can be achieved by using amines,[7,8] MOFs,[9–13] and filters,[14] these processes consume extra energy. To the best of our knowledge, the electrocatalytic reduction of CO_2 at low concentration has not been reported yet.

There are several reports of metal complexes being used to fix low concentration CO_2. Orchin *et al.* determined that CO_2 insertion into the Mn–O bond of *fac*-[Mn(CO)$_3$(P–P)(OEt)] (P–P: diphenylphosphino ethane) to generate *fac*-[Mn(CO)$_3$(P–P){OC(O)OEt}] was possible using pure CO_2 gas as well as air.[15] Umakoshi *et al.* reported the formation of a methyl carbonate complex from [Ru(CNC)(bpy)(OMe)](PF$_6$) (CNC: 2,6-bis(*tert*-butylimidazol-2-ylidene)pyridine) in ambient air.[16]

Recently, we reported the CO_2-capturing ability of a Re(I) complex with deprotonated triethanolamine as a monodentate ligand, *i.e.*, *fac*-[Re(bpy)(CO)$_3${$OC_2H_4N(C_2H_4OH)_2$}] (bpy = 2,2′-bipyridine), to react with CO_2, giving the aminoethylcarbonato complex *fac*-[Re(bpy)(CO)$_3${$OC(O)OC_2H_4N(C_2H_4OH)_2$}] (Scheme 1).[17] Since this equilibrium reaction has a large equilibrium constant ($K = 1.7 \times 10^3$ M^{-1}), *fac*-[Re(bpy)(CO)$_3${$OC_2H_4N(C_2H_4OH)_2$}] can efficiently capture low concentration CO_2. 93% of the Re complex can be converted to the aminoethylcarbonato complex by bubbling Ar gas containing only 10% CO_2 through the solution containing the Re complex.

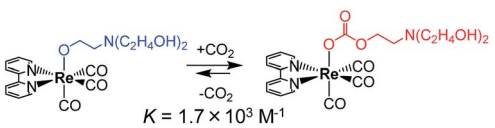

Scheme 1 CO_2 capture by *fac*-[Re(bpy)(CO)$_3${$OC_2H_4N(C_2H_4OH)_2$}].

Department of Chemistry, School of Science, Tokyo Institute of Technology, O-okayama 2-12-1-NE-1, Meguro-ku, Tokyo 152-8550, Japan. E-mail: ishitani@chem.titech.ac.jp

† Electronic supplementary information (ESI) available: Curve fitting of the FT-IR spectrum under 1% CO_2 in DMF–TEOA, detailed cyclic voltammograms of the Re(I) complex, picture of the setup for the bulk electrolysis, time courses of current in the bulk electrolysis, results of the analysis (FT-IR, CVs, and UHPLCs) after electrolysis for experiments under 1% CO_2 in DMF and under 10% CO_2 in DMF–TEOA, and FT-IR spectra of the Re complex before and after adding TPAHBF$_4$. See DOI: 10.1039/c8sc04124e

‡ These authors contributed equally to this work.

§ Present address: Faculty of Science and Technology, Department of Materials and Life Science, Seikei University, 3-3-1 Kichijojikitamachi, Musashino, Tokyo, 180-8633, Japan.

In addition, Re(I) diimine carbonyl complexes having a *fac*-[Re(N^N)(CO)$_3$X] structure are well-known catalysts for CO_2 reduction in electrochemical systems.[18–24] By combining these catalytic and CO_2-capturing properties, the construction of a catalytic system, which can directly utilize low concentration CO_2 as a substrate for CO_2 reduction could be expected.

Herein, we report the electrochemical reduction of low concentration CO_2 with high selectivity, high faradaic efficiency, and good durability using a Re(I) mononuclear complex with CO_2-capturing ability.

Results and discussion

First, we confirmed the ability of the Re(I) complex to capture CO_2 to form the aminoethylcarbonato complex in co-existence with a supporting electrolyte (Et_4NBF_4) for electrochemical reactions (Scheme 2). The *fac*-[Re(dmb)(CO)$_3$(MeCN)]$^+$ (**Re-MeCN$^+$**: dmb = 4,4′-dimethyl-bpy) complex was selected as a starting complex, which can be converted to the ligand substituted complex *fac*-[Re(dmb)(CO)$_3$(DMF)]$^+$ (**Re-DMF$^+$**: DMF = *N*,*N*′-dimethylformamide) by dissolving in a DMF solution containing Et_4NBF_4 (0.1 M), due to the lower stability of the isolated **Re-DMF$^+$**. Part of this DMF complex was converted into a complex with a deprotonated triethanolamine ligand, *i.e.*, *fac*-[Re(dmb)(CO)$_3${OC$_2$H$_4$N(C$_2$H$_4$OH)$_2$}] (**Re-TEOA**) by adding triethanolamine (TEOA) to the DMF solution (DMF : TEOA = 5 : 1 v/v). Fig. 1(a) shows the stretching vibrational bands of the CO ligands of **Re-DMF$^+$** (ν_{CO} = 2028 cm^{-1}, 1921 cm^{-1}, and 1910 cm^{-1}) and **Re-TEOA** (ν_{CO} = 2005 cm^{-1}, 1895 cm^{-1}, and 1878 cm^{-1}) in the mixed solution under an Ar atmosphere. The ratio of **Re-DMF$^+$** and **Re-TEOA** was calculated to be 1 : 2.4 by curve fitting and changed according to the concentration of TEOA; therefore, this ligand substitution reaction is in equilibrium (eqn (1)).

$$\textbf{Re-DMF}^+ + 2\text{TEOA} \rightleftarrows \textbf{Re-TEOA} + \text{TEOA-H}^+ + \text{DMF} \quad (1)$$

On introducing pure CO_2 into the solution (bubbling for 1 min), all the ν_{CO} bands of **Re-DMF$^+$** and **Re-TEOA** disappeared and a set of three new peaks appeared at ν_{CO} = 2019 cm^{-1}, 1913 cm^{-1}, and 1890 cm^{-1}. Fig. 1(b) shows the ν_{CO} bands in Ar containing various concentrations of CO_2. This clearly indicates that CO_2 insertion into the Re–O bond is also in equilibrium (eqn (2)).

$$\textbf{Re-TEOA} + CO_2 \rightleftarrows \textbf{Re-CO}_2\textbf{TEOA} \quad (2)$$

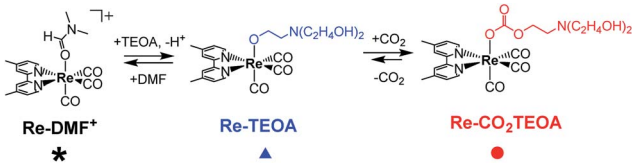

Scheme 2 Ligand substitution and CO_2 capture by the Re(I) complex in a DMF–TEOA mixed solution.

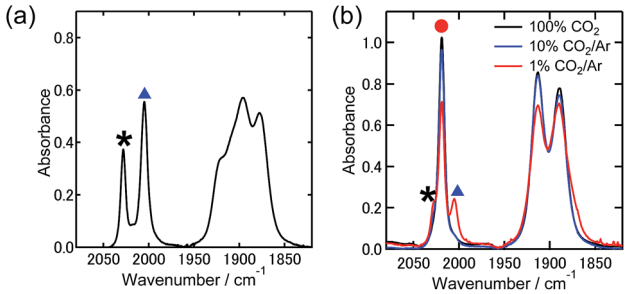

Fig. 1 FT-IR spectra of the Re(I) complexes (5.0 mM) in a DMF–TEOA (5 : 1 v/v) solution containing 0.1 M Et_4NBF_4 after purging with Ar (a), and Ar containing various concentrations of CO_2 (b). Black asterisk (*), blue triangle (▲) and red circle (●) display the peaks which correspond to **Re-DMF$^+$**, **Re-TEOA**, and **Re-CO$_2$TEOA**, respectively.

Analysis of these data using eqn (1) and (2) supplied the equilibrium constants of both reactions as $K_1 = (6.4 \pm 0.2) \times 10^{-2}$ in eqn 1 and $K_2 = (1.6 \pm 0.1) \times 10^3$ M^{-1} in eqn (2). This clearly shows that **Re-TEOA** has high CO_2 capturing ability even in the presence of 0.1 M Et_4NBF_4. We note that a similar value ($K_2 = (1.8 \pm 0.1) \times 10^3$ M^{-1}) was obtained in the absence of the electrolyte. Table 1 summarizes the distribution of the proportions of these complexes under 1% and 10% CO_2 atmospheres. Notably, 67% of the Re(I) complex existed as **Re-CO$_2$TEOA** even under a 1% CO_2 atmosphere (curve-fittings are shown in Fig. S1†), where the solution contains only 2.2 mM CO_2 while the saturating concentration of CO_2 is 0.14 M.[25] Thus, we can assume that the CO_2 capturing property of **Re-TEOA** is applicable to the electrochemical reduction of low concentration CO_2.

Fig. 2 shows the cyclic voltammograms (CVs) of the Re(I) complex(es) in DMF and in a DMF–TEOA (5 : 1 v/v) mixed solution containing the electrolyte, which were measured both under an Ar and a CO_2 atmosphere. Under an Ar atmosphere, the CV of **Re-DMF$^+$** in DMF shows a chemically quasi-reversible reduction wave ($E_{1/2}$ = −1.66 V) attributed to an electron injection into the π* orbital of the diimine ligand of **Re-DMF$^+$**, and a subsequent irreversible reduction wave at E_p = −1.8 V, which is attributed to the reduction of the metal center Re(+/0)[19] (Fig. 2(a), further details in the ESI (Fig. S2(a)†). Under a CO_2 atmosphere, **Re-DMF$^+$** shows a catalytic current at a more negative potential than the second reduction wave.

In the DMF–TEOA mixed solution, both **Re-DMF$^+$** and **Re-TEOA** are present under an Ar atmosphere, as described above. Certainly, the CV of this solution showed a broader "first" reduction wave at E = −1.6 to −1.9 V (Fig. 2(b), and a detailed

Table 1 Distribution of the proportions of the Re(I) complexes in a DMF–TEOA (5 : 1 v/v) solution containing 0.1 M Et_4NBF_4 after purging with Ar containing various concentrations of CO_2

	Re-DMF$^+$	**Re-TEOA**	**Re-CO$_2$TEOA**
100% CO_2	Trace	Trace	>99%
10% CO_2	3%	3%	94%
1% CO_2	15%	18%	67%

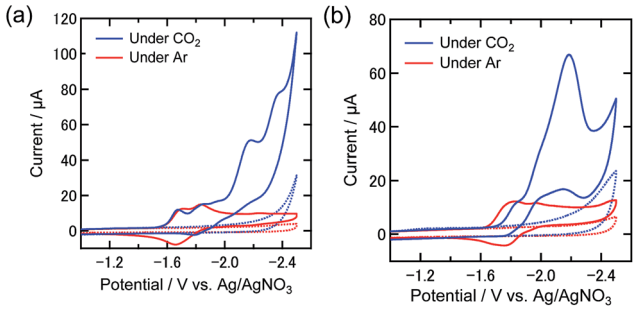

Fig. 2 CVs of the Re(I) complex(es) (total 0.5 mM) (a) in DMF and (b) in the DMF–TEOA (5 : 1 v/v) mixed solution, containing Et_4NBF_4 (0.1 M) as the supporting electrolyte at a sweep rate of 200 mV s^{-1}. Blue and red lines show the CVs under CO_2 and Ar, respectively. Dotted lines indicate CVs for the corresponding solutions without the Re(I) complex. A glassy carbon electrode (diameter: 3 mm), an $Ag/AgNO_3$ (10 mM) electrode and a Pt wire were used as working, reference, and counter electrodes, respectively.

CV in Fig. S2(b)†), which should contain two reduction waves, one from each Re complex; the reduction potential of **Re-TEOA** should be more negative than that of **Re-DMF**$^+$ because of the charge difference. Conversely, under a CO_2 atmosphere, the onset potential of the first reduction wave was shifted by about 70 mV to a more negative value ($E_p = -1.8$ V) because the Re complexes should be converted to **Re-CO_2TEOA** which has no charge. The cathodic catalytic wave was obtained when the sweeping potential was slightly negative of the first reduction wave. It should be noted that the onset potential of this catalytic wave ($E \sim -1.82$ V) was almost the same as in the case for **Re-DMF**$^+$ in the CO_2-purged DMF solution (Fig. 2(a)).

The catalytic current decreased at lower concentrations of CO_2 as shown in Fig. 3(a). In the case of 1% CO_2, the "first" reduction wave was slightly different compared to the other two cases. This reduction could also be caused by the presence of **Re-DMF**$^+$ in addition to **Re-CO_2TEOA** and **Re-TEOA**. Fig. 3(b) shows the relationship between the catalytic current at −1.95 V and the square root of the dissolved CO_2 concentration. This good linearity suggests that the diffusion of CO_2 as a substrate is a rate-determining step in the electrochemical reaction at −1.95 V.[26] In contrast, the current at −1.82 V was almost independent of the concentration of CO_2. This suggests that the rate-determining step of the electrochemical reaction occurring at this potential is not dependent on the concentration of CO_2. From these results we decided to quantitate the products from bulk electrolysis at −1.82 V under 100%, 10%, and 1% CO_2 atmospheres.

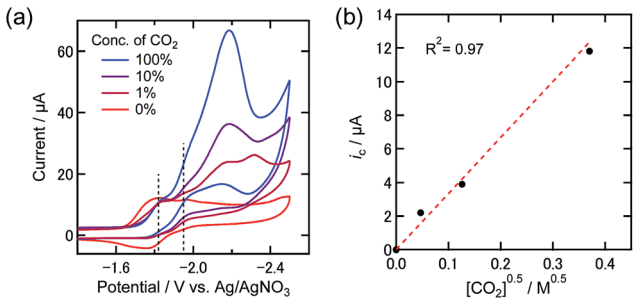

Fig. 3 (a) CVs of the Re(I) complex (0.5 mM) in a DMF–TEOA mixed solution (5 : 1 v/v) containing Et_4NBF_4 (0.1 M) under 100% (blue), 10% (purple), and 1% (maroon) CO_2 atmospheres and under an Ar atmosphere (red). The sweep rate was 200 mV s^{-1}. A glassy carbon electrode (diameter: 3 mm), an $Ag/AgNO_3$ (10 mM) electrode and a Pt wire were used as working, reference, and counter electrodes, respectively. (b) Relationship between the catalytic current at −1.95 V and the square root of the dissolved CO_2 concentration.

An H-shaped electrolytic cell, in which the reduction and oxidation chambers are partitioned by a proton exchange membrane, was used for the electrocatalytic reaction (Fig. S3†). A DMF–TEOA (5 : 1 v/v) solution containing a 0.5 mM Re(I) complex and Et_4NBF_4 (0.1 M) as an electrolyte was added to the cathodic chamber, while the solution for the anodic chamber contained the electrolyte and tetrabutylammonium acetate (TBAOAc) as an electron donor. A potential of −1.82 V *vs.* the $Ag/AgNO_3$ (10 mM) reference electrode was applied to a carbon mesh working electrode for 24 h, while bubbling with Ar gas containing various concentrations of CO_2. Fig. 4(a) shows the time courses of the electrolysis products under 100% CO_2 in a solution in which most of the Re(I) complex was converted to **Re-CO_2TEOA**. A substantially stable reductive current of about 1.3 mA was observed for 24 h (Fig. S4(a)†), and CO was produced as the main reduction product with very small amounts of H_2

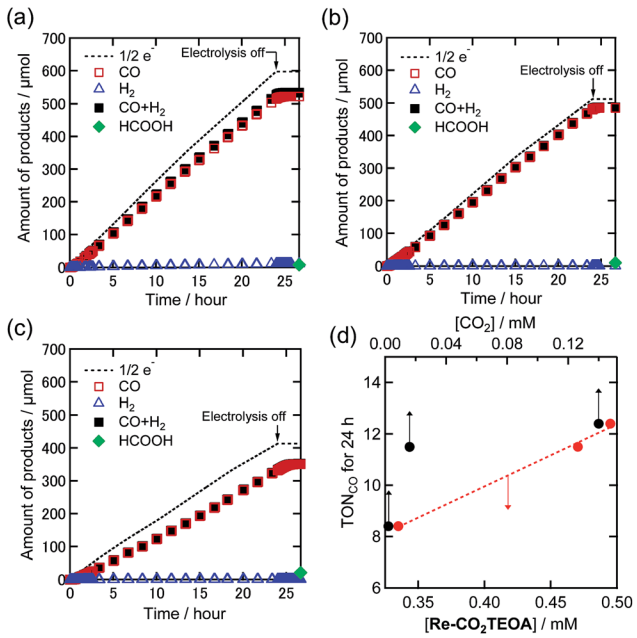

Fig. 4 Time courses of the generation of CO (red square), H_2 (blue triangle), and formic acid (green diamond) with half of the electrons flowing (dotted line) during bulk electrolysis using the Re(I) catalyst (0.5 mM) at −1.82 V in a DMF–TEOA solution containing Et_4NBF_4 (0.1 M) under (a) 100%, (b) 10%, and (c) 1% CO_2 atmospheres (10 mL min^{-1}). Total amounts of CO and H_2 are also indicated by black squares. (d) The relationships of TON_{CO} for a 24 h reaction with the concentrations of **Re-CO_2TEOA** in the solution (red circle) and CO_2 (black circle). Corresponding time courses of the current during bulk electrolysis are shown in Fig. S4.†

and HCOOH as byproducts. The faradaic efficiency (η) of each product was η_{CO} = 87%, η_{H2} = 2% and η_{HCOOH} = 1%. The turnover number for the formation of CO (TON_{CO}) was 12.4 after the 24 h electrolysis and the speed of CO formation did not slow down during the electrolysis.

Fig. 4(b) and (c) show the time courses of the electrolysis products under 10% and 1% CO_2, respectively. Under 10% CO_2 where 91% of the Re(I) complex exists as **Re-CO_2TEOA**, the Re(I) complex still maintained excellent catalytic activity similar to that under 100% CO_2 (η_{CO} = 95%, TON_{CO} = 11.5, and selectivity of CO formation = 98% after 24 h electrolysis). Even when the concentration of CO_2 was lowered to only 1%, a stable reduction current and the corresponding catalytic CO generation were observed with a high faradaic efficiency (η_{CO} = 85%). The TON_{CO} was 8.4 after 24 h electrolysis, which was lower than under 10% and 100% CO_2 atmospheres. Notably, the dissolved CO_2 concentrations in the DMF–TEOA mixed solution using 10% and 1% CO_2 were 16 mM and 2.2 mM, respectively, which are much lower than under a 100% CO_2 atmosphere (140 mM).[17,25] It is noteworthy that TEOA cannot accumulate CO_2 although diethanolamine and ethanolamine can capture CO_2 giving carbamate (R_1R_2NCOOH).[8] However, the electrocatalytic CO_2 reduction by using the Re(I) complex proceeded to generate CO selectively, and the generation rate was maintained at 93% for 10% CO_2 and at 67% for 1% CO_2 compared to that for 100% CO_2. Fig. 4(d) shows the relationship between the TON_{CO} after 24 h electrolysis and the concentration of **Re-CO_2TEOA** (red) and the concentration of CO_2 (black) in the reaction solution. The concentration of **Re-CO_2TEOA** indicates a good linearity with the TON_{CO}, while the concentration of dissolved CO_2 did not show such a good correlation. These results strongly suggest that **Re-CO_2TEOA** electrocatalyzed the CO_2 reduction through the reduction of CO_2 captured by the complex.

Additionally, the electrolysis at −1.76 V under 10% CO_2 was conducted to confirm the onset of the reduction of low concentration CO_2. Fig. 5(a) and (b) display the magnified CV of the Re complex under 10% CO_2 in the DMF–TEOA mixed solution and the time courses of the electrolysis products at −1.76 V under 10% CO_2, respectively. Even at a more positive potential in the first reduction wave, a highly selective and catalytic reaction proceeded (η_{CO} = 84%, TON_{CO} = 4.1, and selectivity of CO formation = 98% after 24 h electrolysis). This concludes that **Re-CO_2TEOA** efficiently electrocatalyzes CO_2 reduction to produce CO with high selectivity even at its first reduction potential under low concentration of CO_2.

To investigate the role of TEOA, electrocatalytic CO_2 reduction was carried out in a DMF solution containing **Re-DMF$^+$** and Et_4NBF_4 as the electrolyte in the absence of TEOA under 100% CO_2 and 1% CO_2 atmospheres. The applied potential was −1.82 V *vs.* $Ag/AgNO_3$ which corresponds to the second reduction wave of **Re-DMF$^+$** (Fig. 2(a)). Fig. 6 shows the time courses of the generation of the products. Under the 100% CO_2 atmosphere, the observed current in the initial stage was greater than that in the presence of TEOA; 4.6 mA was observed (1.5 mA in the presence of TEOA) because the two-electron reduction of **Re-DMF$^+$** proceeded (Fig. S5(a)†). However, it drastically decreased during the first 60 min, and became 0.27 mA after 24 h electrolysis with the corresponding selective CO production (Fig. 6(a)). The faradaic efficiency of CO was 51%, which was much lower than that in the presence of TEOA. Although the **Re-DMF$^+$** has three CO ligands, the TON of the CO formation was less than three. It is noteworthy that the saturated concentration of CO_2 in DMF (0.20 M) was higher than that in the DMF–TEOA (5 : 1 v/v) mixed solution.[27] Under the 1% CO_2 atmosphere, the faradaic efficiency of CO formation was very low even in the initial stage of the electrolysis (Fig. 6(b) and S5(b)†). The TON for CO formation was 0.6 after electrolysis for 24 h. The CV and FT-IR spectrum measured after the electrolysis (Fig. S6†) clearly indicate that most of the Re complex had decomposed to electrochemically inactive species. In a nutshell, **Re-DMF$^+$** did not work as an electrocatalyst under these reaction conditions. From these results, we can conclude that the electrocatalytic reduction of low concentration CO_2 does not proceed in DMF in the absence of TEOA.

It has been reported that the addition of a proton source to the reaction solution sometimes accelerates the electrocatalytic

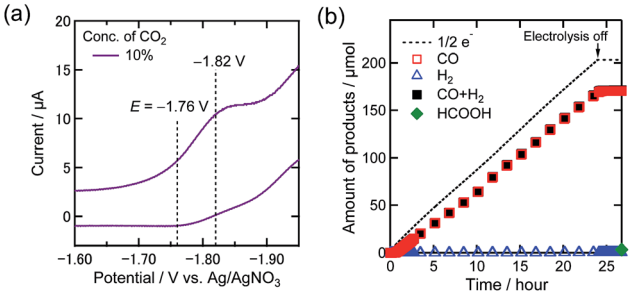

Fig. 5 (a) CV of the Re(I) complex (0.5 mM) in a DMF–TEOA mixed solution (5 : 1 v/v) containing Et_4NBF_4 (0.1 M) under a 10% CO_2 atmosphere. Measurement conditions were the same as those in Fig. 3. (b) Time courses of the generation of CO (red square), H_2 (blue triangle), and formic acid (green diamond) with half of the electrons flowing (dotted line) during bulk electrolysis using the Re(I) catalyst (0.5 mM) at −1.76 V in a DMF–TEOA solution containing Et_4NBF_4 (0.1 M) under a 10% CO_2 atmosphere (10 mL min^{-1}).

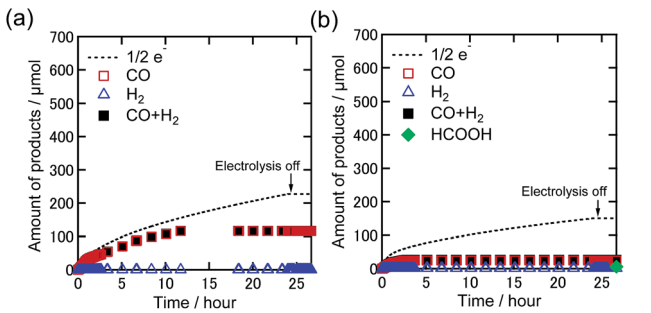

Fig. 6 Time courses of the generation of CO (red square), H_2 (blue triangle), sum of CO and H_2 (black-filled square), and formic acid (green diamond) with half of the electrons flowing (dotted line) during bulk electrolysis using **Re-DMF$^+$** (0.5 mM) at −1.82 V in a DMF solution containing Et_4NBF_4 (0.1 M) under (a) 100% and (b) 1% CO_2 atmospheres (10 mL min^{-1}). Corresponding time courses of the current during bulk electrolysis are shown in Fig. S5.†

CO_2 reduction because the protons work as O^{2-} receptors from the two-electron reduced CO_2 (eqn (3)).[28,29]

$$2CO_2 + 2e^- + H^+ \rightarrow CO + HCO_3^- \quad (3)$$

Since in the current system there is a possibility that the reduction of low concentration CO_2 could proceed due to the effect of the hydroxy protons of TEOA, the addition of tri(*n*-propyl) ammonium tetrafluoroborate ($TPAHBF_4$) as a proton source into the reaction solution instead of TEOA was investigated. Since alcohols possibly form a corresponding CO_2 adduct complex by coordinating to the Re complex, $TPAHBF_4$ which itself and the deprotonated form of which have low coordinating ability to the Re center was used as a proton source. The IR spectrum did not change on adding $TPAHBF_4$ (25 mM) to a DMF solution containing **Re-DMF**$^+$ (5.0 mM) and Et_4NBF_4 (0.1 M) under an Ar atmosphere (Fig. S7†), suggesting that the Re(I) complex does not undergo a ligand substitution reaction with $TPAHBF_4$.

From the CV of the DMF solution containing $TPAHBF_4$ (25 mM) and 0.5 mM **Re-DMF**$^+$ under an Ar atmosphere, an irreversible reduction wave around −1.6 V and a following large catalytic reduction wave starting from around −1.9 V were observed (Fig. 7(a)). The reduction current near −1.9 V could be assigned to the catalytic generation of H_2 catalyzed by the reductive derivatives from **Re-DMF**$^+$. Two-electron reduction of **Re-DMF**$^+$ should eliminate the DMF ligand, and it would react with a proton to generate *fac*-[Re(dmb)(CO)$_3$H] (**Re-H**), which reacts with another proton producing H_2. Fig. 7(b) shows the CVs of the same solution in the presence of 1% and 100% CO_2, where the CV measured under the Ar atmosphere is also shown. Under the 100% CO_2 atmosphere, the first reduction wave around −1.6 V showed no obvious change regardless of the existence of CO_2, while a new reduction wave was observed between −1.8 V and −2 V. Under the 1% CO_2 atmosphere, on the other hand, the CV was similar to that measured under the Ar atmosphere, especially at potentials more positive than −1.9 V.

We conducted bulk electrolysis experiments of the DMF solutions containing $TPAHBF_4$ (25 mM) and 0.5 mM **Re-DMF**$^+$ at E_{BE} = −1.82 V *vs.* Ag/$AgNO_3$ under 100% CO_2 and 1% CO_2 atmospheres. Fig. 8 shows the time courses of product generation during electrolysis. In the case of the 100% CO_2 atmosphere, CO was mainly produced with η_{CO} = 64% and TON_{CO} = 16.3 after 24 h electrolysis (Fig. 8(a)), indicating the progress of the electrocatalytic reduction of CO_2. The faradaic efficiencies of H_2 and HCOOH were η_{H2} = 1% and η_{HCOOH} = 17%, respectively (TON_{H2} = 0.2, TON_{HCOOH} = 4.4). Under the 1% CO_2 atmosphere, on the other hand, no CO production was observed, while catalytic amounts of H_2 (TON_{H2} = 6.1, η_{H2} = 35%) and HCOOH (TON_{HCOOH} = 6.1, η_{HCOOH} = 27%) were produced (Fig. 8(b)). These results clearly indicate that although the proton source accelerates CO_2 reduction at a high concentration of CO_2, it does not assist CO formation *via* reduction of low concentration CO_2. It is interesting that formate was catalytically produced even by using the Re complex as a catalyst because most of the reported electrocatalytic systems using Re(I) complexes as catalysts selectively produced CO but not the formate species even in the presence of proton sources.[30–32] It should be considered that only pure CO_2 was used in these reports.

Table 2 summarizes the bulk electrolysis results. The electrocatalysis of the Re complexes strongly depended on the reaction conditions as described above. Under 100% CO_2, the catalytic formation of CO was the main reaction (entries 1, 5 and 7), and the co-existence of the proton source, *i.e.*, TEOA or $TPAHBF_4$, accelerated the rates of CO formation (entries 1 and 7). At low concentrations of CO_2 (entries 3, 6 and 8), the presence of TEOA in the reaction solution was essential for CO formation. Even at a more positive potential (E = −1.76 V) in the first reduction wave, a highly selective catalytic reaction proceeded (entry 4). It should be noted that the proton source did not positively affect the CO formation in the 1% CO_2 atmosphere. These results also clearly indicate that the CO_2 capturing ability of **Re-TEOA** to yield **Re-CO$_2$TEOA** is essential for the reduction of low concentration CO_2.

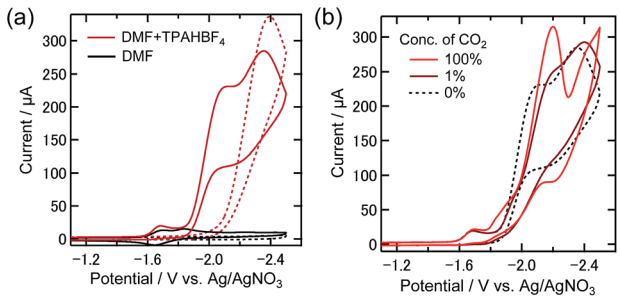

Fig. 7 (a) CVs of **Re-DMF**$^+$ (0.5 mM) in Ar-purged DMF with (red) or without (black line) 25 mM $TPAHBF_4$ as a proton source (dashed line: without **Re-DMF**$^+$). (b) CVs of **Re-DMF**$^+$ (0.5 mM) in the solution containing 100% CO_2 (red), 1% CO_2 (maroon line), and pure Ar (black dotted line). The solutions contain Et_4NBF_4 (0.1 M) as the supporting electrolyte. The sweep rate was 200 mV s^{-1}. A glassy carbon electrode (diameter: 3 mm), an Ag/$AgNO_3$ (10 mM) electrode and a Pt wire were used as working, reference, and counter electrodes, respectively.

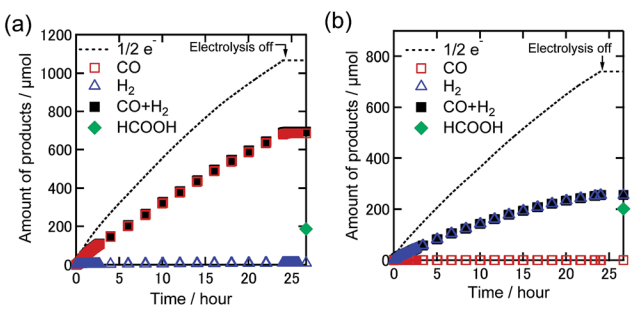

Fig. 8 Time courses of the generated CO (red square), H_2 (blue triangle), sum of CO and H_2 (black-filled square), and formic acid (green diamond) with half of the electrons flowing (dotted line) during bulk electrolysis using **Re-DMF**$^+$ (0.5 mM) at −1.82 V in the DMF solution containing Et_4NBF_4 (0.1 M) and $TPAHBF_4$ (25 mM) under (a) 100% and (b) 1% CO_2 atmospheres (10 mL min^{-1}). Corresponding time courses of the current during bulk electrolysis are shown in Fig. S8.†

Table 2 Reduction products during constant potential electrolysis[a]

	Additive	Conc. of CO_2/%	Consumed electrons/μmol	Products/μmol (TON based on the Re complex)			Faradaic efficiency/%		
				CO	H_2	HCOOH	CO	H_2	HCOOH
1	TEOA	100	1195	522 (12.4)	11.9 (0.28)	8 (0.2)	87	2.0	1
2	TEOA	10	1025	485 (11.5)	1.2 (0.03)	10 (0.2)	95	0.2	2
3	TEOA	1	826	351 (8.4)	0.8 (0.02)	21 (0.5)	85	0.2	5
4[b]	TEOA	10	203	170 (4.1)	0.5 (0.01)	3 (0.1)	84	0.3	2
5	—	100	454	116 (2.8)	0.4 (0.01)	n.d.	51	0.2	~0
6	—	1	300	25 (0.6)	1.7 (0.04)	6 (0.1)	17	1.2	4
7	$TPAHBF_4$	100	2132	685 (16.3)	9 (0.2)	186 (4.4)	64	1	17
8	$TPAHBF_4$	1	1482	n.d.	256 (6.1)	201 (4.8)	~0	35	27

[a] Solutions containing the Re complex (0.5 mM) and Et_4NBF_4 (0.1 M) under $E_{BE} = -1.82$ V *vs.* $Ag/AgNO_3$ for 24 h. [b] Electrolysis under $E_{BE} = -1.76$ V *vs.* $Ag/AgNO_3$ for 24 h. n.d.: not detected.

To clarify any changes in the Re complexes during electrolysis, IR spectra, CVs, and liquid chromatograms of the reaction solutions using an ODS column (UHPLC) were recorded before and after the electrolysis. In the case of the DMF–TEOA mixed solution under the 100% CO_2 atmosphere, *i.e.*, only **Re-CO_2-TEOA** was in solution before electrolysis, no obvious change of the ν_{CO} bands in the IR spectrum was observed even after the electrolysis for 24 h (Fig. 9(a)). In the CV, the shape was unchanged and the reduction current attributed to the Re complexes was slightly reduced after electrolysis (Fig. 9(b)). In UHPLC, the main peak attributed to the starting Re complexes was observed, where the axial ligands of **Re-CO_2TEOA** should be substituted by MeOH and/or H_2O in the mobile phase of the liquid chromatography (Fig. 9(c)). In addition, a smaller peak attributable to the formate complex (*fac*-[Re(dmb)$(CO)_3${OC(O)H}], **Re-OCHO**) was observed, in 13% conversion yield. 0.9% of the total electrons were consumed in the formation of **Re-OCHO**, *i.e.*, $\eta_{FE} = 0.9\%$ since formation of formate from CO_2 requires two electrons. Notably, since the ν_{CO} bands and the CV of **Re-OCHO** are very similar to those of **Re-CO_2TEOA**, the UHPLC analyses were required for the detection of **Re-OCHO**. The same analyses were carried out in the case using 10% CO_2 and showed similar results. The starting Re complexes were detected as the main component by UHPLC and **Re-OCHO** was produced in a 4% yield ($\eta_{FE} = 0.3\%$, Fig. S9(c)†). In the case using 1% CO_2, on the other hand, the yield of **Re-OCHO** increased to 24% ($\eta_{FE} = 2.4\%$, Fig. 10). It has been reported that formate complexes are formed through electrochemical

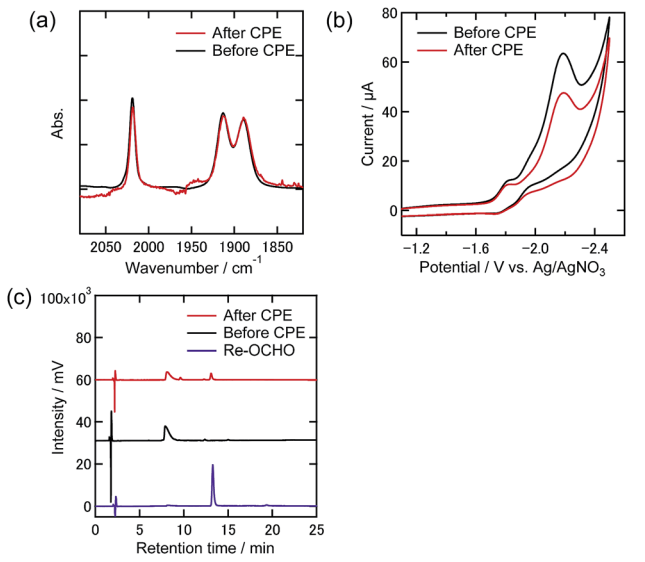

Fig. 9 (a) FT-IR spectra, (b) CVs, and (c) UHPLCs of the Re(I) complexes before and after the electrolysis at −1.82 V under a 100% CO_2 atmosphere in DMF–TEOA containing Et_4NBF_4 (0.1 M) as the supporting electrolyte (black lines: before electrolysis, red lines: after electrolysis). The FT-IR spectra and CVs were measured by using the reaction solutions without any treatment. UHPLC: an ODS column: $\lambda_{det} = 400$ nm, a MeOH–H_2O mixed solution containing KH_2PO_4 buffer of pH 5.9 (1 : 1 v/v) was used as the eluent. The blue line shows the analysis result of the isolated **Re-OCHO** as a reference.

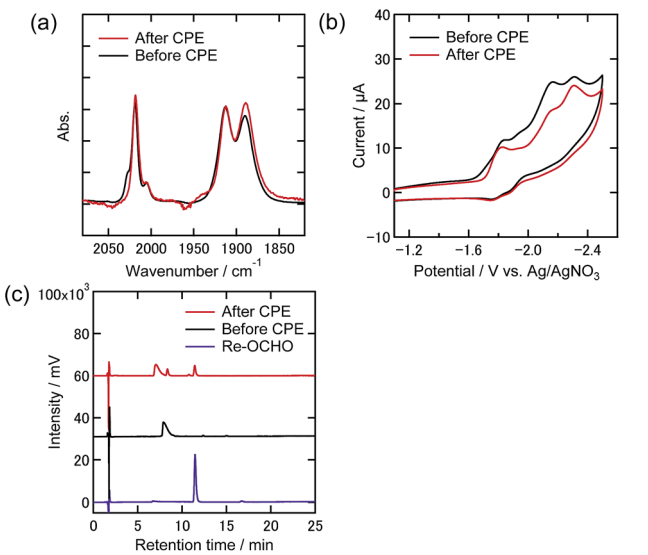

Fig. 10 (a) FT-IR spectra, (b) CVs, and (c) UHPLCs of the Re(I) complexes before and after electrolysis at −1.82 V under a 1% CO_2 atmosphere in DMF–TEOA containing Et_4NBF_4 (0.1 M) as the supporting electrolyte (black lines: before electrolysis, red lines: after electrolysis). Measurement conditions were the same as those in Fig. 9.

CO_2 reduction using *fac*-[Re(N^N)$(CO)_3$L] type complexes as catalysts by CO_2 insertion into the hydride complexes (*fac*-[Re(N^N)$(CO)_3$H]) which are two-electron reduction products of the starting Re complexes.[33,34] In the present system, the coordinatively unsaturated complex might be generated through the reduction of **Re-DMF$^+$** and/or **Re-TEOA** and might react with a proton to produce **Re-H**. Since it has also been reported that desorption of HCO_2^- from the formate complexes *via* their one-electron reduction proceeded,[35] the production of formate in the present electrocatalytic systems may be produced *via* similar processes. It should be noted that the formation reactions of **Re-OCHO** and HCOOH are very minor processes in the whole electrolysis. These results clearly show that during electrolysis the Re complexes acted as stable catalysts even under the 1% CO_2 atmosphere.

In the IR spectra recorded just after electrolysis under the 10% CO_2 and 1% CO_2 atmospheres, **Re-TEOA** was observed in the ratio of 6% and 18% in all complexes (Fig. S9(a)† and 10(a)), while **Re-DMF$^+$** was not. This was also confirmed from their CVs (Fig. S9(b)† and 10(b)). These observations can be explained because the reaction solution should become more basic during electrolysis because the reductive conversion of CO_2 to CO leads to the formation of bicarbonate species as well (eqn (3)). This should move the equilibrium between **Re-DMF$^+$** and **Re-TEOA** to the **Re-TEOA** side. Thus, these results reveal that most of the Re(I) complexes were maintained even after electrolysis at low concentrations of CO_2 for 24 h except for the formation of **Re-OCHO**.

Similar analyses of the electrolyzed solutions containing $TPAHBF_4$ instead of TEOA were conducted (Fig. 11 and 12). Although the CO formation rates were very different between the 100% and 1% CO_2 atmospheres as described above (entries 7 and 8 in Table 2), the UHPLC and FT-IR spectra after the electrolysis were similar to each other. In the UHPLC, the peak attributed to **Re-OCHO** was mainly observed (Fig. 11(b) and 12(b)). The conversion yields based on the **Re-DMF$^+$** used were 73% (100% CO_2) and 64% (1% CO_2), respectively. The FT-IR results also supported that most of the **Re-DMF$^+$** was converted to **Re-OCHO**; only the peaks attributed to **Re-OCHO** were observed at ν_{CO} = 2017 cm^{-1}, 1912 cm^{-1}, and 1888 cm^{-1}.

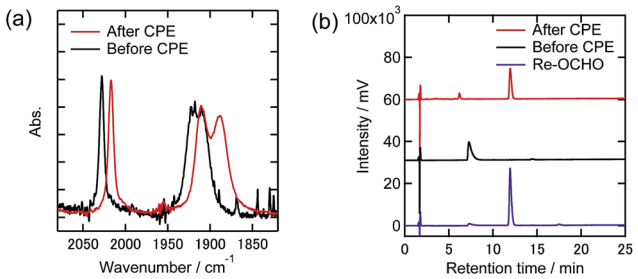

Fig. 11 (a) FT-IR spectra and (b) UHPLCs of the Re(I) complexes before and after electrolysis at −1.82 V with the existence of $TPAHBF_4$ (25 mM) under a 100% CO_2 atmosphere in DMF–TEOA containing Et_4NBF_4 (0.1 M) as the supporting electrolyte (black lines: before electrolysis, red lines: after electrolysis). Measurement conditions were the same as those in Fig. 9.

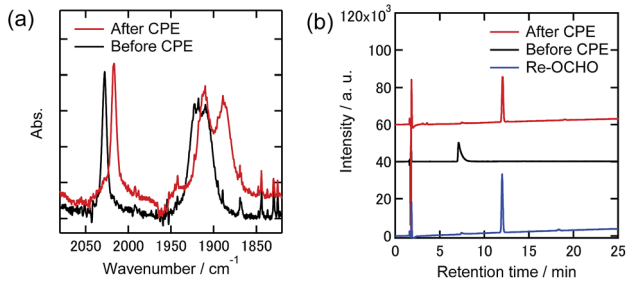

Fig. 12 (a) FT-IR spectra and (b) UHPLCs of the Re(I) complexes before and after electrolysis at −1.82 V with the existence of $TPAHBF_4$ (25 mM) under a 1% CO_2 atmosphere in DMF–TEOA containing Et_4NBF_4 (0.1 M) as the supporting electrolyte (black lines: before electrolysis, red lines: after electrolysis). Measurement conditions were the same as those in Fig. 9.

Therefore, it was concluded that **Re-DMF$^+$** was converted to **Re-OCHO** during electrolysis in the presence of $TPAHBF_4$. These results also suggest that **Re-H** was generated as an intermediate during electrolysis and insertion of CO_2 into the **Re-H** bond gave **Re-OCHO**. It is noteworthy that, even under the 1% CO_2 atmosphere, the **Re-DMF$^+$** was converted in good yield and HCOOH was catalytically produced (TON_{HCOOH} = 4.8 after 24 h electrolysis). Therefore, the electrochemical formation of formate from a low concentration of CO_2 by the Re complexes is possible.

Experimental

Materials

DMF was dried with 4 Å molecular sieves for several days and then distilled under reduced pressure. TEOA was distilled under vacuum. These compounds were stored under an Ar atmosphere before use. The electrolyte, Et_4NBF_4 was recrystallized from MeCN/ethyl acetate, and then dried under vacuum at 373 K overnight before use. Other reagents and solvents were of commercial grade quality and were used without further purification.

Synthesis

fac-Re(dmb)$(CO)_3$Br was synthesized according to a previously reported method.[36]

***fac*-[Re(dmb)$(CO)_3$(MeCN)](PF_6) (Re-MeCN$^+$).** An MeCN solution containing Re(dmb)$(CO)_3$Br (0.677 g, 1.27 mmol) and $AgPF_6$ (0.323 g, 1.28 mmol) was refluxed in the dark overnight, and then exposed to room light for 1 h. After precipitation, AgBr was removed by filtration with Celite, and the solution was evaporated under reduced pressure. The residual solid was dissolved in an NH_4PF_6-saturated mixed solution (MeCN/H_2O = 1 : 1 v/v). MeCN was evaporated slowly to precipitate the product as a yellow powder. Yield: 0.771 g (95%). FT-IR (in MeCN) ν_{CO}/cm^{-1}: 2040, 1935. ESI-MS (in MeCN): *m*/*z*: 496 $[M - PF_6^-]^+$. Anal. calcd for $C_{17}H_{15}N_3F_6O_3PRe$: C, 31.88; H, 2.36; N, 6.56. Found: C, 31.60; H, 2.24; N, 6.73. ^{1}H NMR (400 MHz, CD_3CN, ppm) δ = 8.83 (d, 2H, J = 5.5 Hz, H6, 6′), 8.33 (br, 2H, H3, 3′), 7.54 (dd, 2H, J = 5.5, 1.0 Hz, H5, 5′), 2.05 (s, 6H, CH_3).

***fac*-[Re(dmb)(CO)$_3$(DMF)](PF$_6$) (Re-DMF$^+$).** A DMF solution (70 mL) containing **Re-MeCN** (26.9 mg, 42 μmol) was kept at room temperature for 3 h under an Ar atmosphere and dim light. FT-IR (in DMF) ν_{CO}/cm^{-1}: 2028, 1921, 1911.

***fac*-[Re(dmb)(CO)$_3${OC(O)H}] (Re-OCHO).** A H_2O–EtOH mixed solution (1 : 1 v/v, 50 mL) containing *fac*-[Re(CO)$_3$(dmb)Br] (0.320 g, 0.599 mmol) and NaOCHO (4.01 g, 60.0 mmol) was refluxed overnight under dim light. The solution was slowly evaporated under reduced pressure until all of the EtOH was removed. Extraction with dichloromethane was performed three times. The organic phase was evaporated under reduced pressure. The residual yellow solid was recrystallized from water–acetone, and then dried overnight under vacuum at 333 K. Yield: 0.182 g (61%). FT-IR (in CH_2Cl_2): ν_{CO}/cm^{-1}: 2017, 1912, 1888. ^{1}H NMR (400 MHz, $CDCl_3$, ppm) δ = 8.97 (d, 2H, J = 5.6 Hz, H6, 6′), 8.10 (d, 1H, CHO), 7.95 (br, 2H, H3, 3′), 7.33 (dd, 2H, J = 5.6, 1.2 Hz, H5, 5′), 2.57 (s, 6H, CH_3).

Tri-*n*-propylammonium tetrafluoroborate (TPAHBF$_4$). A HBF_4 aqueous solution (42%, 85 mL) was added to the 200 mL plastic flask. *n*-tripropylamine (105 mL, 0.53 mol) was added dropwise to the solution at 273 K to obtain a white solid. After the solid was filtered, the crude product was recrystallized from ethyl acetate and dried under vacuum at room temperature overnight before use. Yield: 44.7 g (36.5%). ESI-MS (in MeCN): *m*/*z*: 144 [M − BF_4^-]$^+$, ^{1}H-NMR (400 MHz, $CDCl_3$, ppm) δ = 3.09–3.04 (m, 6H, N–CH_2), 1.83–1.74 (m, 6H, –CH_2–CH_3), 1.03 (t, J = 7.3 Hz, 9H, –CH_3).

General procedure

^{1}H NMR spectra were recorded in $CDCl_3$ or CD_3CN on a JEOL ECA400-II system at 400 MHz. Transmission IR spectra in CH_2Cl_2 or the reaction solution were recorded on a JASCO FT/IR-610 or FT/IR-6600 spectrometer at 1 cm^{-1}. Electrospray ionization-mass spectroscopy (ESI-MS) was performed using a Shimadzu LC-MS-2010 A system with MeCN as the mobile phase. Solutions containing 5 mM complexes and 0.1 M Et_4NBF_4 were prepared for the FT-IR measurements, and a solution containing only 0.1 M Et_4NBF_4 was used for the background measurements. Ultra high performance chromatograms (UHPLC) of the Re complexes were recorded on a SHIMADZU UHPLC Nexera X2 with an ODS column (Waters Acquity: 150 mm × 2.1 mm i.d.), a Shimadzu DGU-20A degasser, an LC-30AD pump, an SPD-M30A UV-vis photodiode-array detector, and a Rheodyne 7125 injector. The eluent was a 1 : 1 (v/v) mixture of methanol and water containing 0.05 M KH_2PO_4 (pH 5.9), and the flow rate was 0.2 mL min^{-1}.

Calculation of equilibrium constants

We conducted preparation procedures of the solutions for the measurements in a glove box (UNICO, UN-650F) combined with a gas circulation dehydration device (DGE-05) under Ar (water content was less than 376 ppm). We obtained concentrations of the complexes in solution, using the peak areas of ν_{CO} at the highest wavenumber (2000–2060 cm^{-1}) in the IR spectra. The peak areas for each complex were obtained by curve-fitting using a linear combination of the Gaussian and the Lorentzian functions using the bundled software (JASCO Spectra Manager II Software).[25] For the calculation of K_1 in eqn (1) (ligand substitution reaction), **Re-MeCN$^+$** (10.0 mM) was dissolved in DMF (0.5 mL) and this solution was kept at room temperature in the dark for several hours (>3 h) to convert **Re-MeCN$^+$** into **Re-DMF$^+$** completely. After adding a DMF solution (0.5 mL) containing TEOA (2.48 M) and Et_4NBF_4 (0.2 M) to this solution, the mixed solution was kept at room temperature in the dark for 2 h (the concentration of the total Re complex, TEOA and Et_4NBF_4 is 5.0 mM, 1.26 M and 0.1 M, respectively) and the IR spectra of the equilibrium mixtures **Re-MeCN$^+$** and **Re-TEOA** were measured. The K_1 value was calculated using eqn (4) and the obtained concentrations of each Re(I) complex. This experiment was repeated three times, and the average value and the standard deviation were obtained.

$$K_1 = \frac{[\textbf{Re-TEOA}][\mathrm{DMF}][\text{H-TEOA}^+]}{[\textbf{Re-DMF}^+][\mathrm{TEOA}]^2} \approx \frac{[\textbf{Re-TEOA}]^2[\mathrm{DMF}]}{[\textbf{Re-DMF}^+][\mathrm{TEOA}]^2} \quad (4)$$

For the calculation of K_2 in eqn (2) (CO_2-capture reaction), **Re-MeCN$^+$** (6.0 mM) was dissolved in DMF (1.0 mL) and this solution was kept at room temperature in the dark for several hours (>3 h). After adding 1.0 mL of a DMF solution containing TEOA (2.52 M) and Et_4NBF_4 (0.2 M) to this solution, the mixed solution was kept at room temperature in the dark for 2 h (the concentration of the total Re complex, TEOA and Et_4NBF_4 is 3.0 mM, 1.26 M and 0.1 M respectively at this time). Then, a CO_2-saturated DMF solution (30 μL, the CO_2 concentration is 0.20 M)[27] was added to this mixed solution in a shielded tube (the volume of this tube is 2.0 mL) by using a micro-syringe in a glove box. After keeping at room temperature in the dark for 2 h, the IR spectra were measured. The K_2 value was calculated using eqn (5) and the obtained concentrations of each Re(I) complex. This experiment was also repeated three times, and the average value and the standard deviation were obtained.

$$K_2 = \frac{[\textbf{Re-CO}_2\textbf{TEOA}]}{[\textbf{Re-TEOA}][\mathrm{CO_2}]} \quad (5)$$

Cyclic voltammetry

CV measurements were performed using a typical three electrode configuration with an ALS CHI-760e potentiostat. The experiments were carried out in a vessel containing *ca.* 5 mL of a sample solution using a glassy carbon disk (diameter = 3 mm) as the working electrode. An Ag/$AgNO_3$ electrode (Ag wire immersed in DMF containing 0.01 M $AgNO_3$ and 0.1 M Et_4NBF_4, separated from the chamber by vycol® glass) was used as a reference electrode. The platinum wire was employed as a counter electrode.

Bulk electrolysis

Bulk electrolysis was carried out in an H-shaped electrochemical cell (Fig. S3†) with a Hokuto Denko HZ-7000 potentiostat using a reticulated vitreous carbon mesh (RVC®, 20 PPI,

$2.0 \times 2.5 \times 0.64$ cm^3 volume immersed in the solution) as the working electrode. An $Ag/AgNO_3$ electrode (Ag wire immersed in DMF containing 0.01 M $AgNO_3$ and 0.1 M Et_4NBF_4, separated from the chamber by vycol® glass) was used as a reference electrode. The platinum grid was employed as a counter electrode, which was divided from the cathodic chamber by a Nafion® perfluorinated membrane (Nafion® 324, Aldrich). The reference electrode was placed close to the working electrode so as to minimize the ohmic drop. The working electrode was washed with acetone and dried for 3 h in a vacuum, and then electrochemically pre-reduced at −1.82 V over 3 h in DMF solution containing only the Et_4NBF_4 electrolyte in the same atmosphere as the desired reaction. The cathodic chamber was filled with an 84 mL portion of the complex solution. The anodic chamber was filled with 84 mL of the DMF–TEOA solution (5 : 1 v/v) which contained the electrolyte and tetrabutylammonium acetate (TBAOAc) as an electron donor. Before measurement, the cathodic chamber had been purged with the gas containing a specific concentration of CO_2, while the anodic chamber had been purged with Ar over 1 h. The cathodic chamber of the electrochemical cell was attached to the gas flow system. The gas flow was controlled by a mass flow controller, and the possibility of the effect of back pressure can be negligible since the gas pressure in the upstream was only 0.2 MPa and that in the downstream should be 1 atm, which was released to the ambient pressure. The solution had been continuously bubbled with Ar gas containing various concentrations of CO_2 (100%, 10%, 1%, and 0%), and the headspace of the reaction space had been continuously exchanged by the steady rate of the conveyer gas. The gas products (CO and H_2) from the reaction space in the vented conveyer gas were detected by using a gas chromatograph (Agilent 490 micro-GC) equipped with a thermal conductivity detector. HCOOH in the liquid phase was detected by Photal CAPI-3300I capillary electrophoresis after each reaction. The amount of the produced HCOOH by the electrolysis was calculated by subtracting the HCOOH amount produced in the control solution from that in the electrolyzed solution. The control solution was kept at room temperature for the same period as the bulk electrolysis. The amounts of formic acid produced in the control solution were much less than those produced by the electrolysis, for example, the produced amount of formic acid by the electrolysis with $TPAHBF_4$ was 186 μmol under 100% CO_2 and 201 μmol under 1% CO_2 while 0.82 μmol under 100% CO_2, and 2.72 μmol under 1% CO_2 in the reference solution.

Conclusions

The electrochemical reduction of low concentration CO_2 by using Re(I) complexes as catalysts was systematically investigated. The results clearly show that the CO_2 capturing ability of **Re-TEOA** is very useful for CO formation *via* the reduction of low concentration CO_2, such as 1%. In the absence of TEOA, on the other hand, the Re(I) complexes cannot reduce low concentration CO_2 to CO. In the presence of a proton donor which is not an alcohol, the Re(I) complexes cannot work as electrocatalysts for CO formation under low concentration CO_2. Under these conditions, however, **Re-DMF**$^+$ was converted to **Re-OCHO** *via* CO_2 insertion into the electrochemically produced **Re-H**, and formate was catalytically produced even at low concentrations of CO_2.

Conflicts of interest

There are no conflicts to declare.

Acknowledgements

This work was supported by JST CREST Grant Number JPMJCR13L1 in "Molecular Technology". We acknowledge Prof. Marc Robert (Université Paris Diderot) and Prof. Alain Deronzier (Universite Joseph Fourier) for useful discussion.

Notes and references

1 E. E. Benson, C. P. Kubiak, A. J. Sathrum and J. M. Smieja, *Chem. Soc. Rev.*, 2009, **38**, 89–99.
2 C. D. Windle and R. N. Perutz, *Coord. Chem. Rev.*, 2012, **256**, 2562–2570.
3 C. Finn, S. Schnittger, L. J. Yellowlees and J. B. Love, *Chem. Commun.*, 2012, **48**, 1392–1399.
4 C. Costentin, M. Robert and J. M. Saveant, *Chem. Soc. Rev.*, 2013, **42**, 2423–2436.
5 K. A. Grice and C. P. Kubiak, in *CO2 Chemistry*, eds.M. Aresta and R. van Eldik, Academic Press, 2014, vol. 66, pp. 163–188.
6 G. V. Last and M. T. Schmick, *Environ. Earth Sci.*, 2015, **74**, 1189–1198.
7 A. B. Rao and E. S. Rubin, *Environ. Sci. Technol.*, 2002, **36**, 4467–4475.
8 B. Dutcher, M. Fan and A. G. Russell, *ACS Appl. Mater. Interfaces*, 2015, **7**, 2137–2148.
9 R. Banerjee, A. Phan, B. Wang, C. Knobler, H. Furukawa, M. O'Keeffe and O. M. Yaghi, *Science*, 2008, **319**, 939–943.
10 J. An and N. L. Rosi, *J. Am. Chem. Soc.*, 2010, **132**, 5578–5579.
11 G.-P. Hao, W.-C. Li, D. Qian, G.-H. Wang, W.-P. Zhang, T. Zhang, A.-Q. Wang, F. Schüth, H.-J. Bongard and A.-H. Lu, *J. Am. Chem. Soc.*, 2011, **133**, 11378–11388.
12 Q. Wang, J. Luo, Z. Zhong and A. Borgna, *Energy Environ. Sci.*, 2011, **4**, 42–55.
13 S. Horike, K. Kishida, Y. Watanabe, Y. Inubushi, D. Umeyama, M. Sugimoto, T. Fukushima, M. Inukai and S. Kitagawa, *J. Am. Chem. Soc.*, 2012, **134**, 9852–9855.
14 S. D. Kenarsari, D. Yang, G. Jiang, S. Zhang, J. Wang, A. G. Russell, Q. Wei and M. Fan, *RSC Adv.*, 2013, **3**, 22739–22773.
15 S. K. Mandal, D. M. Ho and M. Orchin, *Organometallics*, 1993, **12**, 1714–1719.
16 Y. Arikawa, T. Nakamura, S. Ogushi, K. Eguchi and K. Umakoshi, *Dalton Trans.*, 2015, **44**, 5303–5305.
17 T. Morimoto, T. Nakajima, S. Sawa, R. Nakanishi, D. Imori and O. Ishitani, *J. Am. Chem. Soc.*, 2013, **135**, 16825–16828.
18 J. Hawecker, J.-M. Lehn and R. Ziessel, *J. Chem. Soc., Chem. Commun.*, 1984, 328–330.

19 B. P. Sullivan, C. M. Bolinger, D. Conrad, W. J. Vining and T. J. Meyer, *J. Chem. Soc., Chem. Commun.*, 1985, 1414–1416.
20 J. M. Smieja and C. P. Kubiak, *Inorg. Chem.*, 2010, **49**, 9283–9289.
21 J. Hawecker, J.-M. Lehn and R. Ziessel, *Helv. Chim. Acta*, 1986, **69**, 1990–2012.
22 J. Agarwal, E. Fujita, H. F. Schaefer and J. T. Muckerman, *J. Am. Chem. Soc.*, 2012, **134**, 5180–5186.
23 M. D. Sampson, J. D. Froehlich, J. M. Smieja, E. E. Benson, I. D. Sharp and C. P. Kubiak, *Energy Environ. Sci.*, 2013, **6**, 3748–3755.
24 A. Nakada and O. Ishitani, *ACS Catal.*, 2017, **8**, 354–363.
25 T. Nakajima, Y. Tamaki, K. Ueno, E. Kato, T. Nishikawa, K. Ohkubo, Y. Yamazaki, T. Morimoto and O. Ishitani, *J. Am. Chem. Soc.*, 2016, **138**, 13818–13821.
26 J. M. Smieja and C. P. Kubiak, *Inorg. Chem.*, 2010, **49**, 9283–9289.
27 H. Konno, A. Kobayashi, K. Sakamoto, F. Fagalde, N. E. Katz, H. Saitoh and O. Ishitani, *Inorg. Chim. Acta*, 2000, **299**, 155–163.
28 K. Y. Wong, W. H. Chung and C. P. Lau, *J. Electroanal. Chem.*, 1998, **453**, 161–169.
29 N. P. Liyanage, H. A. Dulaney, A. J. Huckaba, J. W. Jurss and J. H. Delcamp, *Inorg. Chem.*, 2016, **55**, 6085–6094.
30 K.-Y. Wong, W.-H. Chung and C.-P. Lau, *J. Electroanal. Chem.*, 1998, **453**, 161–170.
31 J. M. Smieja, E. E. Benson, B. Kumar, K. A. Grice, C. S. Seu, A. J. M. Miller, J. M. Mayer and C. P. Kubiak, *Proc. Natl. Acad. Sci. U. S. A.*, 2012, **109**, 15646–15650.
32 J. A. Keith, K. A. Grice, C. P. Kubiak and E. A. Carter, *J. Am. Chem. Soc.*, 2013, **135**, 15823–15829.
33 B. P. Sullivan and T. J. Meyer, *J. Chem. Soc., Chem. Commun.*, 1984, 1244–1245.
34 B. P. Sullivan and T. J. Meyer, *Organometallics*, 1986, **5**, 1500–1502.
35 F. P. A. Johnson, M. W. George, F. Hartl and J. J. Turner, *Organometallics*, 1996, **15**, 3374–3387.
36 C. Bruckmeier, M. W. Lehenmeier, R. Reithmeier, B. Rieger, J. Herranz and C. Kavakli, *Dalton Trans.*, 2012, **41**, 5026–5037.